Thermodynamic properties of strongly interacting matter in a finite volume using the Polyakov–Nambu–Jona-Lasinio model

Abhijit Bhattacharyya[*]

Department of Physics, University of Calcutta, 92, A. P. C. Road, Kolkata 700 009, India

Paramita Deb[†]

Physical Research Laboratory, Theory Division, Navarangpura, Ahmedabad 380 009, India

Sanjay K. Ghosh[‡] and Rajarshi Ray[§]

Department of Physics and Centre for Astroparticle Physics and Space Science, Bose Institute, 93/1, A. P. C. Road, Kolkata 700 009, India

Subrata Sur[‖]

Department of Physics, Panihati Mahavidyalaya, Barasat Road, Sodepur, Kolkata 700 110, India

We present the thermodynamic properties of strongly interacting matter in finite volume in the framework of Polyakov loop enhanced Nambu-Jona-Lasinio model within mean field approximation. We considered both the 2 flavor and 2 + 1 flavor matter. Our primary observation was a qualitative change in the phase transition properties that resulted in the lowering of the temperature corresponding to the critical endpoint. This would make it favorable for detection in heavy-ion experiments that intend to create high density matter with considerably small temperatures. We further demonstrate the possibility of obtaining chiral symmetry restoration even within the confined phase in finite volumes.

I. INTRODUCTION

The strongly interacting matter is supposed to have a rich phase structure at finite temperatures and densities [1]. While our Universe at the present epoch contains a significant fraction of color singlet hadrons, color nonsinglet states especially quarks and gluons may have been prevalent in the past—a few microseconds after the big bang [2]. The temperature of the Universe at that epoch is estimated to be ∼200 MeV. A similar state of matter is also expected to exist inside the core of super-massive stars in the present day Universe, where the density is ∼10 times that of normal nuclear matter. A direct study of such natural phenomenon is out of bounds even to modern astrophysicists. Fortunately experimental facilities at CERN (France/Switzerland), BNL (USA) and recently at GSI (Germany) are exploring the possibilities of creating and studying the properties of such exotic states of matter in a controlled environment. The key differences that appear in such experiments as compared to the natural phenomenon are the lifetime of matter created in the exotic state and its volume. Whereas in natural phenomenon the lifetime of the exotic matter may be large compared to the interaction time scale, it is usually very small in an experimental situation.

Some effects of the enhanced lifetime on the physical aspects of the system relating to the onset of equilibrium of weak interactions were discussed by us in Ref. [3]. Here we shall discuss the effects of finite volume on the properties of strongly interacting matter.

In the following we shall generically define the matter with color confined states as the hadronic phase and the exotic state with colored degrees of freedom as the quark-gluon plasma. In the experiments this exotic phase may be produced by ultra relativistic collisions of heavy ions. The volume of the system thus created would depend on the nature of the colliding nuclei, the center of mass energy ($\sqrt{s}$) and the centrality of collision. Once created, the system expands until the constituents are so far separated that their interaction ceases and they flow out as free streaming particles. The distribution of particles thus freezes out, except for some further decays to smaller particles. There have been a large number of efforts to estimate the system size at freeze-out for different $\sqrt{s}$ and different centralities. The most popular way of doing so is to measure the Hanbury-Brown-Twiss radii (see, e.g., Refs. [4,5] for reviews). In Ref. [6] it has been shown that the freeze-out volume increases as the $\sqrt{s}$ increases. Here the authors have estimated the freeze-out volume and found it to vary from 2000 fm³ to 3000 fm³. In a very recent paper [7] the volume of homogeneity has been calculated using UrQMD model [8] and compared with the experimentally available results. The $\sqrt{s}$ considered was in the range of 62.4 to 2760 GeV for lead-lead collisions at different centralities. The system volume has been

[*]abphy@caluniv.ac.in
[†]paramita.deb83@gmail.com
[‡]sanjay@bosemain.boseinst.ac.in
[§]rajarshi@bosemain.boseinst.ac.in
[‖]ssur.phys@gmail.com

found to vary from 50 fm^3 to 250 fm^3. Given that these are the freeze-out volumes, one can trace back to the initial equilibration time and expect an even smaller system size. In fact one cannot even consider the whole fireball, which is an isolated system to be in thermodynamic equilibrium. One has to choose a proper rapidity interval to act as the system under consideration. Therefore it becomes important to study how the various thermodynamic quantities in a strongly interacting matter depend on the volume of the system. Specifically we know that finite system sizes would lead to smoothening of any singularities appearing at a phase transition [9]. Thus important signatures of such transitions must be reanalyzed with the help of finite size scaling analysis [10]. In the context of heavy ion collisions such a possible analysis has been discussed in the literature (see, e.g., Refs. [11–13]).

On the theoretical side a study of finite volume effects was done in Ref. [14] with a bag of noninteracting quarks and gluons and it was found that the effective degrees of freedom are reduced. In Ref. [15] a two model equation of state was used to show that the separation between the hadronic and quark-gluon plasma phases around the critical temperature loses its sharpness resulting in a soft effective equation of state. A few first principle study of pure gluon theory on space-time lattices were performed, showing the possibility of significant finite size effects [16,17]. Similar studies are going on in various QCD inspired models. In Refs. [18,19] the quark mass gap equation has been studied with Schwinger-Dyson equation parallel to equivalent Lattice QCD (LQCD) calculations and various meson properties are found to have significant volume dependence. In the context of chiral perturbation theory the implications of finite system size have been discussed [20,21]. Then there are studies with four-Fermi type interactions, like the Nambu-Jona-Lasinio (NJL) [22] models [11,23,24], linear sigma models [12,25,26] and Gross-Neveu models [27]. While in Ref. [25] the scaling behavior of chiral phase transition for finite and infinite volumes has been studied, the character of phase diagram has been studied in Refs. [11,12,26,27]. In Refs. [23,24] the authors have studied the chiral properties as a function of the radius of a finite droplet of quark matter. The stability of such a droplet in the context of strangelet formation within the NJL model has been addressed in Ref. [28]. Size dependent effects of difermion states within 2-dimensional NJL model has been studied in Ref. [29] and that of magnetic field is discussed in Ref. [30]. Recently in a 1 + 1 dimensional NJL model the induction of charged pion condensation phenomenon in dense baryonic matter due to finite volume effects has been studied in Ref. [31].

In this work we shall use the Polyakov loop enhanced NJL (PNJL) model to study the thermodynamic properties of the strongly interacting matter in a finite volume. This model originated from the NJL model [32–34] which incorporates the global symmetries of QCD quite nicely. A four quark interaction term in the NJL Lagrangian is able to generate the physics of spontaneous breaking of chiral symmetry—a property of QCD which is manifested as the nondegenerate chiral partners of the low-mass hadrons. However a reasonable description of the physics of color confinement is missing. With the introduction of a background field in the NJL model, motivated by the dynamics of the Polyakov Loop [35], one obtains the PNJL model which describes a number of features of confinement physics quite satisfactorily (see e.g., Refs. [36–44]).

Certain aspects of finite volume effects in the PNJL model has been discussed in Ref. [45] through a coarse graining of the Lagrangian, followed by a Monte Carlo simulation. This method goes on similar lines as the numerical studies of LQCD. Normally this would involve the same kind of complex determinant problem that has plagued the direct LQCD computations for nonzero baryon number densities. So it may be desirable to keep using the saddle point approximation in PNJL model to study the finite volume effects. Here we make the first case study, albeit with some simplified assumptions toward that direction.

We organize our paper as follows. In the next section we briefly describe the PNJL model and the modifications for finite volume. In Sec. III we describe phase transition at finite volume and in Sec. IV we discuss the thermodynamic properties. The pion and sigma meson masses and the pion decay constant at finite volume have been discussed in Sec. V. In Sec. VI we summarize and conclude.

II. THE PNJL MODEL

We shall consider the PNJL model with light flavors (2 flavor) and light plus strange flavors (2 + 1 flavor). In the PNJL model the gluon physics comes into play through the chiral point couplings between quarks (present in the NJL part) and a background field which represents Polyakov Loop dynamics. The Polyakov line is represented as,

$$L(\bar{x}) = \mathcal{P} \exp\left[i \int_0^\beta d\tau A_4(\bar{x}, \tau) \right], \quad (1)$$

where $A_4 = iA_0$ is the temporal component of Euclidian gauge field $(\bar{A}, A_4)$, $\beta = \frac{1}{T}$, and $\mathcal{P}$ denotes path ordering. $L(\bar{x})$ transforms as a field with charge one under global Z(3) symmetry. The Polyakov loop is then given by $\Phi = (\mathrm{Tr}_c L)/N_c$, and its conjugate by $\bar{\Phi} = (\mathrm{Tr}_c L^\dagger)/N_c$. The gluon dynamics can be described as an effective theory of the Polyakov loops. The Polyakov loop potential can be expressed as

$$\frac{\mathcal{U}'(\Phi[A], \bar{\Phi}[A], T)}{T^4} = \frac{\mathcal{U}(\Phi[A], \bar{\Phi}[A], T)}{T^4} - \kappa \ln (J[\Phi, \bar{\Phi}]), \quad (2)$$

where $\mathcal{U}(\phi)$ is a Landau-Ginsburg type potential commensurate with the Z(3) global symmetry. Here we choose a form given in Ref. [37],

$$\frac{\mathcal{U}(\Phi, \bar{\Phi}, T)}{T^4} = -\frac{b_2(T)}{2} \bar{\Phi}\Phi - \frac{b_3}{6}(\Phi^3 + \bar{\Phi}^3)$$
$$+ \frac{b_4}{4}(\bar{\Phi}\Phi)^2, \tag{3}$$

where

$$b_2(T) = a_0 + a_1\left(\frac{T_0}{T}\right) + a_2\left(\frac{T_0}{T}\right)^2 + a_3\left(\frac{T_0}{T}\right)^3, \tag{4}$$

b_3 and b_4 being constants. The second term in Eq. (2) is the Vandermonde term which replicates the effect of SU(3) Haar measure and is given by

$$J[\Phi, \bar{\Phi}] = (27/24\pi^2)[1 - 6\Phi\bar{\Phi} + 4(\Phi^3 + \bar{\Phi}^3) - 3(\Phi\bar{\Phi})^2].$$

The corresponding parameters were earlier obtained in the above mentioned literature by choosing suitable values by fitting a few physical quantities as function of temperature obtained in LQCD computations. The set of values chosen here are

$$a_0 = 6.75, \qquad a_1 = -1.95, \qquad a_2 = 2.625,$$
$$a_3 = -7.44, \qquad b_3 = 0.75, \qquad b_4 = 7.5,$$
$$T_0 = 190 \text{ MeV}, \qquad \kappa = 0.2 (\text{for 2 flavor}),$$
$$\kappa = 0.13 (\text{for 2 + 1 flavor}).$$

For the quarks we shall use the usual form of the NJL model except for the substitution of a covariant derivative containing a background temporal gauge field. Thus the 2 flavor version of PNJL model is described by the Lagrangian,

$$\mathcal{L} = \sum_{f=u,d} \bar{\psi}_f \gamma_\mu iD^\mu \psi_f - \sum_f m_f \bar{\psi}_f \psi_f + \sum_f \mu_f \gamma_0 \bar{\psi}_f \psi_f$$
$$+ \frac{g_S}{2} \sum_{a=1,2,3} [(\bar{\psi}\tau^a \psi)^2 + (\bar{\psi}i\gamma_5\tau^a \psi)^2]$$
$$- \mathcal{U}'(\Phi[A], \bar{\Phi}[A], T). \tag{5}$$

For 2 + 1 flavor the Lagrangian may be written as

$$\mathcal{L} = \sum_{f=u,d,s} \bar{\psi}_f \gamma_\mu iD^\mu \psi_f - \sum_f m_f \bar{\psi}_f \psi_f$$
$$+ \sum_f \mu_f \gamma_0 \bar{\psi}_f \psi_f + \frac{g_S}{2} \sum_{a=0,...,8} [(\bar{\psi}\lambda^a \psi)^2$$
$$+ (\bar{\psi}i\gamma_5\lambda^a \psi)^2] - g_D[\det \bar{\psi}_f P_L \psi_{f'}$$
$$+ \det \bar{\psi}_f P_R \psi_{f'}] - \mathcal{U}'(\Phi[A], \bar{\Phi}[A], T), \tag{6}$$

where f denotes the flavors u or d or s, respectively. The matrices $P_{L,R} = (1 \pm \gamma_5)/2$ are respectively the left-handed and right-handed chiral projectors, and the other terms have their usual meaning, described in detail in Refs. [39,41,43,46–48]. This NJL part of the theory is analogous to the BCS theory of superconductor, where the pairing of two electrons leads to the condensation causing a gap in the energy spectrum. Similarly in the

chiral limit, the NJL model exhibits dynamical breaking of $SU(N_f)_L \times SU(N_f)_R$ symmetry to $SU(N_f)_V$ symmetry (N_f being the number of flavors). As a result the composite operators $\bar{\psi}_f \psi_f$ pick up nonzero vacuum expectation values. The quark condensate is given as

$$\langle \bar{\psi}_f \psi_f \rangle = -iN_c \mathcal{L}t_{y \to x^+}(\text{tr}S_f(x - y)), \tag{7}$$

where trace is over color and spin states. The self-consistent gap equation for the constituent quark masses are

$$M_f = m_f - g_S \sigma_f + g_D \sigma_{f+1}\sigma_{f+2}, \tag{8}$$

where $\sigma_f = \langle \bar{\psi}_f \psi_f \rangle$ denotes chiral condensate of the quark with flavor f. Here if we consider $\sigma_f = \sigma_u$, then $\sigma_{f+1} = \sigma_d$ and $\sigma_{f+2} = \sigma_s$. Similarly if $\sigma_f = \sigma_d$ then $\sigma_{f+1} = \sigma_s$ and $\sigma_{f+2} = \sigma_u$, if $\sigma_f = \sigma_s$ then $\sigma_{f+1} = \sigma_u$ and $\sigma_{f+2} = \sigma_d$. The expression for σ_f at zero temperature ($T = 0$) and chemical potential ($\mu_f = 0$) may be written as [42]

$$\sigma_f = -\frac{3M_f}{\pi^2} \int^\Lambda \frac{p^2}{\sqrt{p^2 + M_f^2}} dp, \tag{9}$$

Λ being the three-momentum cutoff. This cutoff have been used to regulate the model because it contains dimensionful couplings rendering the model to be nonrenormalizable.

Because of the dynamical breaking of chiral symmetry, $N_f^2 - 1$ Goldstone bosons appear. These are the pions and kaons whose masses, decay widths etc. from experimental observations are utilized to fix the NJL model parameters. The parameter values have been listed in Table I. Here we consider the Φ, $\bar{\Phi}$ and σ_f fields in the mean field approximation where the mean field are obtained by simultaneously solving the respective saddle point equations.

Now that the PNJL model is described for infinite volumes, we discuss how we implement the finite volume constraints. Ideally one should choose the proper boundary conditions—periodic for bosons and antiperiodic for fermions. This would lead to a infinite sum over discrete momentum values $p_i = \pi n_i/R$, where $i = x$, y, z and n_i are all positive integers and R is the lateral size of a cubic volume. This implies a lower momentum cutoff $p_{\min} = \pi/R = \lambda$ (say). One should also incorporate proper effects of surface and curvatures. In this first case study we shall however take up a number of simplifications listed below:

TABLE I.   Parameters of the fermionic part of the model.

Model	m_u MeV	m_s MeV	Λ MeV	$g_S\Lambda^2$	$g_D\Lambda^5$
2 flavor	5.5	0	651	4.27	0
2 + 1 flavor	5.5	134.76	631	3.67	9.33

(i) We shall neglect surface and curvature effects.

(ii) The infinite sum will be considered as an integration over a continuous variation of momentum albeit with the lower cut-off.

(iii) We shall not use any modifications to the mean-field parameters due to finite size effects. Our philosophy had been to hold the known physics at zero T, zero μ and infinite V fixed. That means we treat V as a thermodynamic variable in the same footing as T and μ. Therefore any variation due to change in either of these thermodynamic parameters were translated into the changes in the effective fields of σ_f, Φ etc. and through them to the meson spectra. The values of meson masses and decay constants used to fix the model parameters were thus naturally expected to be the values strictly at $T = 0$ and $\mu = 0$ and $V = \infty$. Thus the Polyakov loop potential as well as the mean-field part of the NJL model would remain unchanged. They shall feel the effect of changing volume only implicitly through the saddle point equations.

III. PHASE TRANSITION

To study the finite volume effects on the thermodynamic properties of strongly interacting matter we begin by writing down the thermodynamic potential in mean field approximation.

The expression is given by

$$\Omega'(\Phi, \bar{\Phi}, \sigma_f, T, \mu_f)$$
$$= \mathcal{U}'[\Phi, \bar{\Phi}, T] + 2g_S \sum_{f=u,d,s} \sigma_f^2 - \frac{g_D}{2}\sigma_u\sigma_d\sigma_s$$
$$- T\sum_n \int_\lambda^\infty \frac{d^3p}{(2\pi)^3} \operatorname{Tr}\ln \frac{S^{-1}(i\omega_n, \bar{p})}{T}, \qquad (10)$$

where $\omega_n = \pi T(2n + 1)$ are Matsubara frequencies for fermions. The inverse quark propagator is given in momentum space by

$$S^{-1} = \gamma_0(p^0 + \hat{\mu} - iA_4) - \vec{\gamma} \cdot \vec{p} - \hat{M} \qquad (11)$$

using the identity $\operatorname{Tr}\ln(X) = \ln\det(X)$, we get

$$\Omega' = \mathcal{U}'[\Phi, \bar{\Phi}, T] + 2g_S \sum_{f=u,d,s} \sigma_f^2 - \frac{g_D}{2}\sigma_u\sigma_d\sigma_s - 6\sum_f \int_\lambda^\Lambda \frac{d^3p}{(2\pi)^3} E_{p_f} \Theta(\Lambda - |\vec{p}|)$$
$$- 2\sum_f T \int_\lambda^\infty \frac{d^3p}{(2\pi)^3} \ln\left[1 + 3\left(\Phi + \bar{\Phi}\exp\left(\frac{-(E_{p_f} - \mu_f)}{T}\right)\right)\exp\left(\frac{-(E_{p_f} - \mu_f)}{T}\right) + \exp\left(\frac{-3(E_{p_f} - \mu_f)}{T}\right)\right]$$
$$- 2\sum_f T \int_\lambda^\infty \frac{d^3p}{(2\pi)^3} \ln\left[1 + 3\left(\bar{\Phi} + \Phi\exp\left(\frac{-(E_{p_f} + \mu_f)}{T}\right)\right)\exp\left(\frac{-(E_{p_f} + \mu_f)}{T}\right) + \exp\left(\frac{-3(E_{p_f} + \mu_f)}{T}\right)\right]$$
$$= \Omega - \kappa T^4 \ln J[\Phi, \bar{\Phi}], \qquad (12)$$

where $E_{p_f} = \sqrt{p^2 + M_f^2}$ is the single quasiparticle energy. In the last line Ω contains all the terms of Ω' except the Vandermonde term.

We now search for the saddle point of the thermodynamic potential which gives the temperature and density dependence of the fields. For all the system sizes, at zero baryon density, we found that the order parameters for both chiral ($\sigma = \langle \bar{u}u \rangle + \langle \bar{d}d \rangle$) and deconfinement ($\Phi$) transition smoothly passes from the hadronic phase to the quark phase. This indicates that the system does not have a real phase transition, rather there is a smooth crossover. The crossover temperature is identified to be the point of inflection of σ_u and Φ with temperature. In Fig. 1 we have plotted $d\Phi/dT$ and $d\sigma_u/dT$ for 2 flavor and $2 + 1$ flavor matter for different system sizes. The peak position of these plots give respective inflection points. Note that, the deconfinement and chiral transitions do not take place exactly at the same temperature. Here we take the average of these two temperatures as T_c. The results are shown in Table II, where we quote the different values of the crossover temperatures corresponding to different system sizes.

From Table II it can be seen that the T_c has a strong dependence on system size. For 2 flavors the T_c varies from 167 to 186 MeV which means a change of about 10%. A similar result is observed for $2 + 1$ flavor. One should note that the shift in the T_c is mainly due to the shift in the transition temperature of the chiral phase transition. The transition temperature of the deconfining phase transition almost does not change. This result is similar to that obtained with PNJL model on the lattice [45]. This is somewhat expected as the Polyakov loop potential feels the effect of changing volume only indirectly through the fields Φ and $\bar{\Phi}$.

In Fig. 2 we have plotted the temperature dependence of the constituent quark masses for both 2 flavors and $2 + 1$ flavors. Below the crossover temperature they exhibit very strong volume dependence. Smaller the volume, smaller is the constituent mass. In the $2 + 1$ flavor case, the masses of the light flavors drop faster than the strange quark. It thus seems that the chiral symmetry is gradually getting restored as one looks into smaller and smaller volumes. This is also the reason why the T_c itself is lowered for smaller volumes given in Table II. A similar feature has
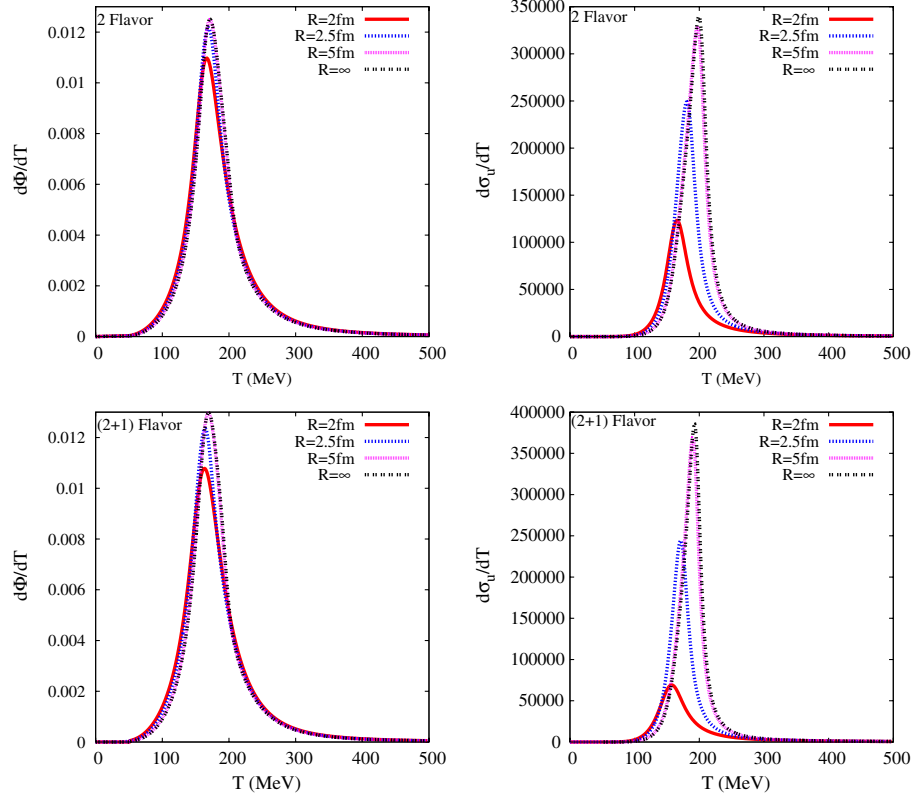
FIG. 1 (color online).   Derivatives of order parameters for chiral and deconfinement phase transition for different system sizes.

also been observed in NJL models [23,24]. Given that the quark condensation is similar to the superconducting condensate it is interesting to note that there are in fact certain superconductors which show similar decrease of band gap with the system size [49].

Let us now take a look into the situation at nonzero quark chemical potential $\mu_q = \sum_f \mu_f / N_f$. For infinite volume the phase transition is of first order and one observes a gap in the order parameter at sufficiently high chemical potential. At some smaller μ_q, the first order transition ends at a critical endpoint (CEP). At this point the system undergoes a second order transition. At even smaller μ_q we have only a crossover. As the volume of the system is lowered we find the phase transition characteristics fade away. Even the crossover characteristics start to die down. This is clear from the Fig. 3 where we plot $d\sigma_u/dT$ and $d\Phi/dT$ for $\mu_q = 300$ MeV as a function of temperature. In Fig. 4 the phase diagram as a function of system size is shown. Note that the CEP gradually shifts towards higher μ_q and lower T and finally disappears as

the volume is reduced. This is an encouraging fact for the critical point search in heavy-ion collision experiments. To attain such high densities one needs to collide the ions at low $\sqrt{s}$, which means the temperature attained is lower. So if it were an infinite system one would have been far away from the CEP. Fortunately the experiments would produce small system volumes and this may lead to the location of the respective CEP possible. Thereafter one would need to do the finite size scaling analysis to extrapolate to the CEP for infinite volumes. The location of CEP for different volumes is collected in Table III.

IV. THERMODYNAMICS

In this section we discuss the behavior of a few thermodynamic observables namely pressure, energy density, specific heat, speed of sound etc. for different system sizes.

The pressure inside a volume V may be written as, $P(T, \mu_q) = -\frac{\partial(\Omega(T,\mu_q)V)}{\partial V}$, where T is the temperature and μ_q is the quark chemical potential. In the top left panel of

TABLE II.   Transition temperatures for different system sizes.

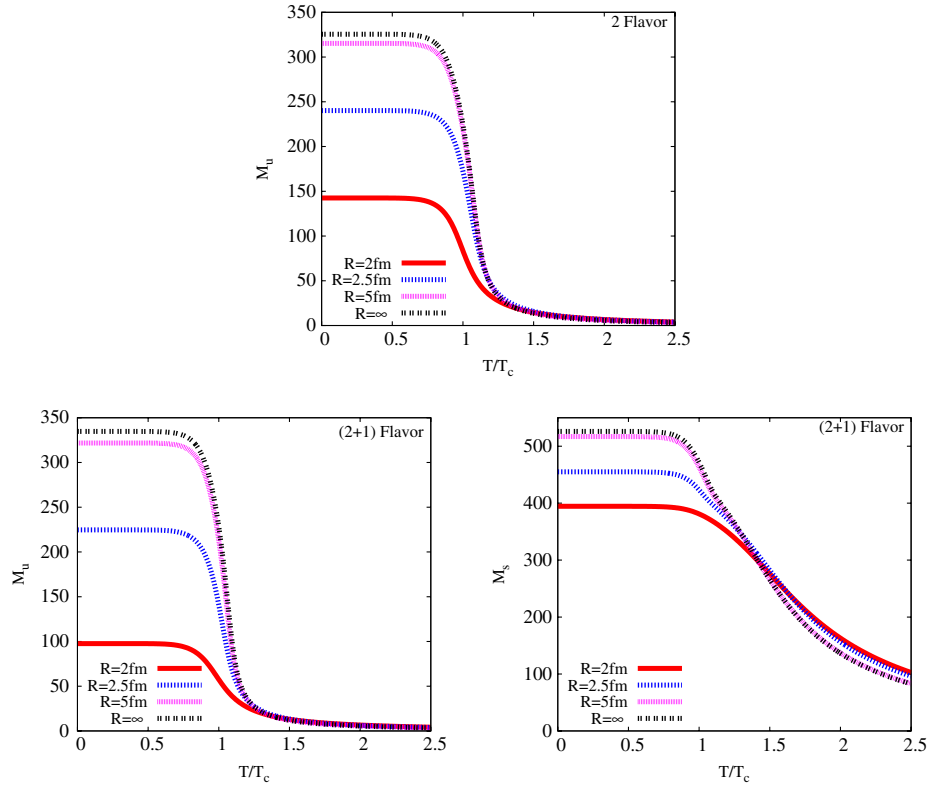|	$R = 2$ fm	$R = 2.5$ fm	$R = 3$ fm	$R = 5$ fm	$R = \infty$
T_c (MeV) (2 flavor)	167	171	180	184	186
T_c (MeV) (2 + 1 flavor)	160	167	174	180	181

FIG. 2 (color online).   Constituent masses of quarks as a function of temperature for different system sizes.

Fig. 5 we plot the temperature dependence of scaled pressure (P/T^4) for a 2 flavor system. As can be seen there is a significant change in scaled pressure for small system sizes. For example at T_c the P/T^4 for a system with $R = 2$ fm is almost half of that of an infinite system. As the temperature increases the difference slowly diminishes. The decrease of scaled pressure with increasing volume may be a surprise given that the constituent quark masses were shown to decrease drastically with decreasing volume, which should imply increase in pressure. This can be understood as follows. With decreasing volume, not only the constituent masses decrease, but also the lowest momentum increases due to the infrared cutoff. These

two conditions somehow seem to keep the lowest available energy of the quark quasi-particles almost the same for different volumes. Thus the pressure does not increase with decreasing volume. However, when plotted against T/T_c it seems to decrease because the T_c itself is smaller for smaller volumes, and therefore the pressure at the corresponding T/T_c for smaller volume is smaller than that for a larger volume.

The volume dependence is also quite strong for the energy density $\epsilon = -T^2 \frac{\partial(\Omega/T)}{\partial T}|_V = -T\frac{\partial\Omega}{\partial T}|_V + \Omega$. In the top right panel of the Fig. 5 we have plotted the ϵ/T^4 as a function of T/T_c for different system sizes. It has similar characteristics as P/T^4 but the difference seems to
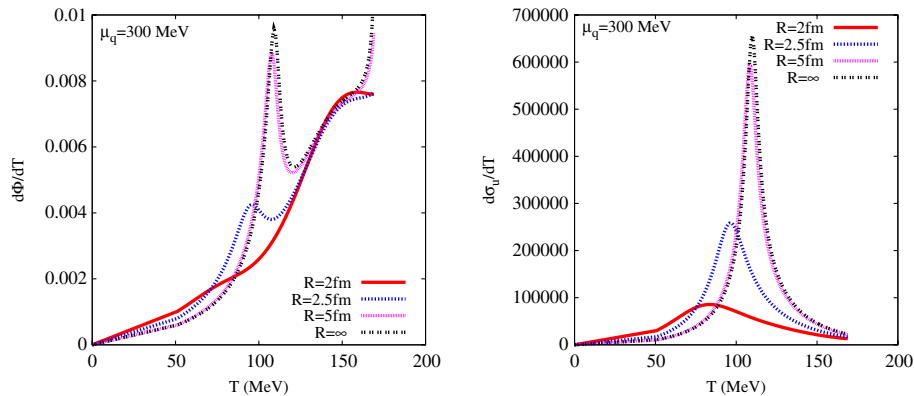

FIG. 3 (color online).   Derivatives of order parameters for chiral and deconfinement phase transition for 2 flavor at finite μ_q.
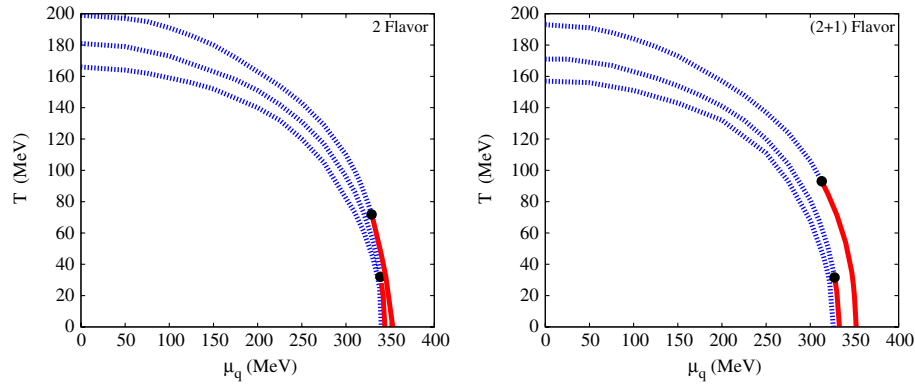
FIG. 4 (color online).   Phase diagram for different system sizes. The inside curve is for $R = 2$ fm, the next curve is for $R = 2.5$ fm and the outermost curve is for $R = \infty$.

diminish faster with increasing temperature. As the system size becomes $R = 5$ fm both the scaled pressure and scaled energy density converge to the $R \to \infty$ case for almost all temperatures.

It is well known that for infinite volumes the definition of pressure simplifies to, $P(T, \mu_q) = -\Omega(T, \mu_q)$, which is commonly used in the literature for PNJL models at infinite volumes. However, since we are considering finite volumes here it would be interesting to check how much difference will it make if we keep using this definition rather than the correct one with a volume derivative. In the bottom two panels of Fig. 5 we have made a comparison of $-\Omega/T^4$ and P/T^4. For $R = 2$ fm we see that these two quantities differ by about 10%. Again, as the size goes close to $R = 5$ fm this difference is almost washed out.

Let us now consider the quantity $\epsilon - 3P$. In our mean field approach this is the trace of the energy-momentum tensor given by, $\mathcal{T}_{\mu\mu} = \epsilon - 3P$. In a conformally symmetric theory, for example a theory of free massless quarks and gluons the energy momentum tensor is supposed to be zero as it signifies the conservation of the conformal currents. Thus $\epsilon = 3P$ in that limit. In QCD however the conformal symmetry is broken due to nonzero quark masses as well as quantum anomalies as evident from the presence of a *scale* in the running coupling constant [50,51]. Thus the energy-momentum tensor does not remain traceless. This was also found to be true in the PNJL models that have been reported in our earlier studies and compared with LQCD results [39,41,46]. The PNJL model is however not QCD and the reason for the scale symmetry breaking is the introduction of an ultraviolet cutoff in the NJL part, a temperature scale T_0 in the Polyakov loop part and of course a quark mass term similar to that in QCD.

The physical implication of the two different scales in the quark and Polyakov sector is to give rise to separate crossover temperatures for the two sectors. To compare quantities obtained in the PNJL model against LQCD results one then averages out two crossover temperatures as done by us here in the last section. Now for finite system sizes we have introduced an infrared cutoff which should further enhance the effect of conformal symmetry breaking. In Fig. 6 we show the variation of the conformal measure $\mathcal{C} = (\epsilon - 3P)/\epsilon$ with temperature for both 2 flavor and and $2 + 1$ flavor matter for different system sizes. That the smaller system sizes lead to larger conformal symmetry breaking effects is evident, except for the anomalous behavior of the lowest size of $R = 2$ fm. (Though not shown in the figure we found that the anomalous behavior starts at a size between 2 fm $\leq R \leq 2.5$ fm. The reason for this behavior is not clear at the moment and requires further investigation.)

The specific heat at constant volume $C_V = \frac{\partial \epsilon}{\partial T}|_V$ is shown in Fig. 7. We find that with the change in volume, C_V changes prominently up to the temperature corresponding to the crossover region. For smaller volumes the specific heat is smaller indicating a higher rise in temperature for the same rise in energy density. Obviously this can be correlated with the temperature dependence of energy density discussed earlier in Fig. 5. We found that a given amount of scaled energy density is obtained at a higher scaled temperature for a smaller volume. This can be of interest in heavy-ion collision experiments. A given energy density deposited in the finite volume would create a plasma with temperature somewhat higher than that expected in a similar volume inside an infinite volume system having the same energy density.

TABLE III.   Location of chiral CEP for different system sizes.

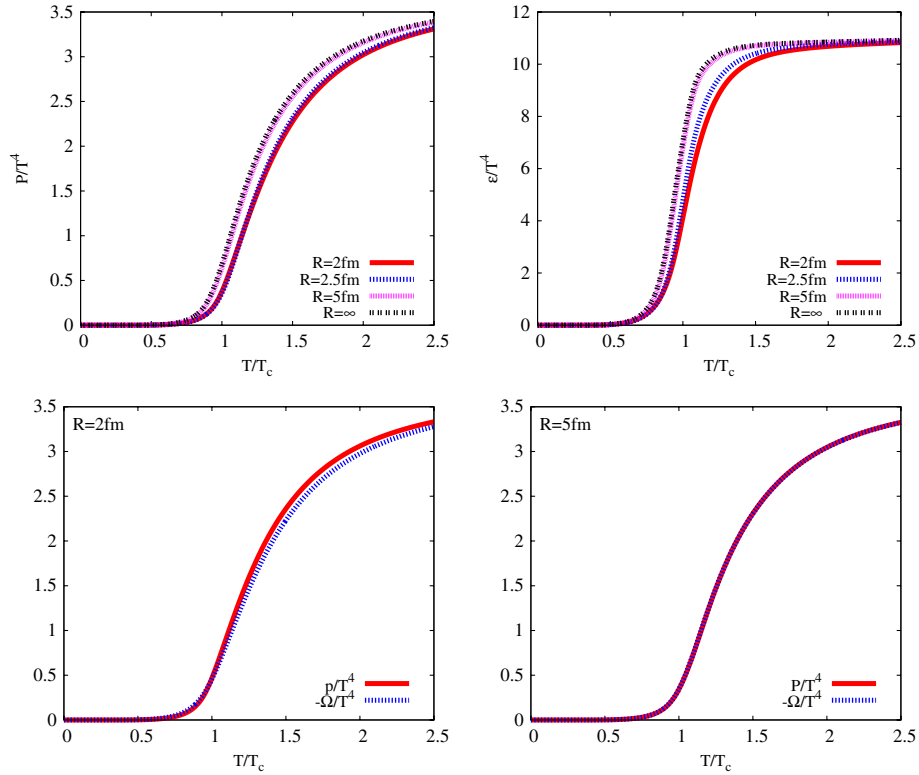|	$R = 2$ fm	$R = 2.5$ fm	$R = 3$ fm	$R = 5$ fm	$R = \infty$
T_c (MeV), μ_{qc} (MeV) (2 flavor)	No CEP	32, 339	52, 335	69, 330	72, 329
T_c (MeV), μ_{qc} (MeV) ($2 + 1$ flavor)	No CEP	32, 328	60, 324	86, 316	93, 313

FIG. 5 (color online).   Pressure and energy density as a function of temperature (top panel). Comparison of pressure and $-\Omega$ (bottom panel). These plots are for 2 flavor matter only.
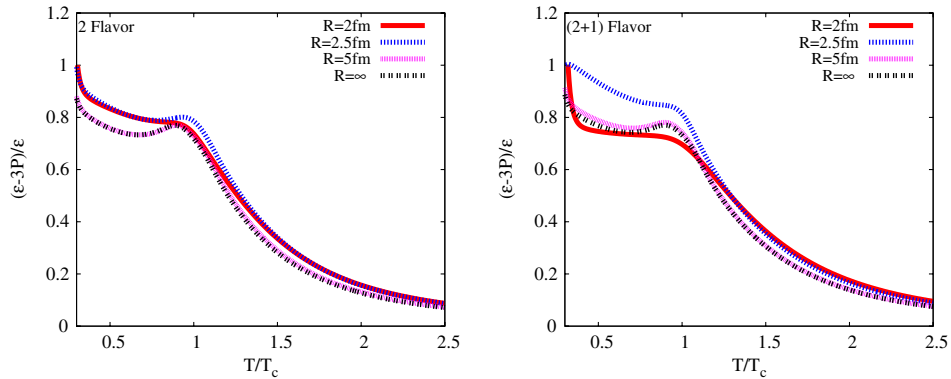

FIG. 6 (color online).   Conformal measure $\mathcal{C} = 1 - 3P/\epsilon$ for different system sizes as a function of temperature.
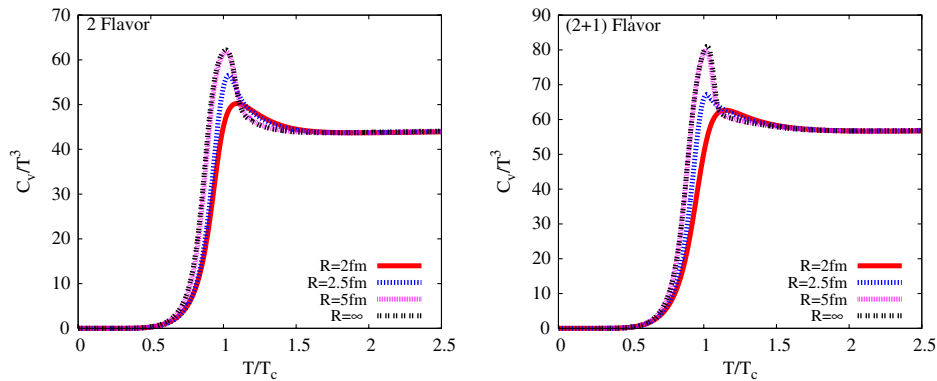

FIG. 7 (color online).   Variation of specific heat with temperature for different system sizes.
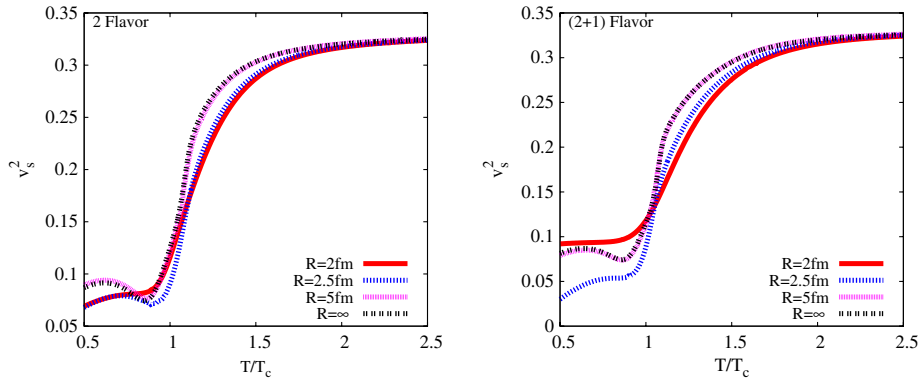
FIG. 8 (color online).   Variation of squared speed of sound with temperature for different system sizes.

The specific heat is also a measure of energy fluctuations in the system [52]. Fluctuations tend to rise sharply near a phase transition. For a crossover they are somewhat subdued. Obviously for finite volumes a true phase transition is not possible and as one keeps on decreasing the volume all signatures even for a crossover should die down. This is exactly the behavior of C_V as presented in Fig. 7.

The squared speed of sound $v_s^2 = \frac{\partial P}{\partial \epsilon}$ is shown in Fig. 8. At large temperatures the v_s^2 reaches its maximum value as the system becomes almost ideal. Interactions grow with decreasing temperatures resulting in the lowering of v_s^2. The conformal measure $\mathcal{C}$ may be considered as a measure of the strength of the interaction in the system. Thus lower the value of $\mathcal{C}$, higher should be the value of v_s^2. This is evident from Fig. 8, where we find the v_s^2 to decrease with decreasing temperature, just opposite to the behavior of $\mathcal{C}$ shown in Fig. 6. This correlation between $\mathcal{C}$ and v_s^2 is also apparent for variation in volume. With decreasing volume the speed of sound decreases. (In fact an anomalous behavior for the smallest size $R = 2$ fm is also apparent for v_s^2). A smaller speed of sound for smaller volumes would mean a slower flow for finite size systems created in heavy-ion collisions.

V. PROPERTIES OF NONSTRANGE MESONS

For infinite volumes the meson properties in the PNJL model has been discussed for 2 flavors [53,54] as well as for $2 + 1$ flavors [43,55]. In this section we describe the properties of nonstrange mesons at finite volumes in the PNJL model. A detailed account of the calculational procedure for meson masses at finite temperatures and densities in the PNJL model may be found in Ref. [43]. Here we sketch the outline of the task.

The collective excitations, the fluctuation of the mean field around the vacuum can be handled within the random phase approximation [56]. In this approximation, which is equivalent to summing over the ring diagrams, the retarded correlation function for a meson M is given by

$$D_M^R = \frac{\Pi^M}{1 - 2G_M\Pi^M}. \tag{13}$$

Here G_M is the suitable coupling constant and $\Pi_M(k^2)$ is the one-loop polarization function for the mesonic channel under consideration. Within the random phase approximation, Π^M may be written as

$$\Pi^M \equiv \int_\lambda^\Lambda \frac{d^4p}{(2\pi)^4} \, \mathrm{Tr}[\Gamma_M S(p+q)\Gamma_M S(q)], \tag{14}$$

where $S(p)$ is the Hartree quark propagator, Γ_M is the appropriate combination of gamma matrices of different mesonic channels and the trace is taken over the Dirac and color spaces. The lower limit on the integration is now required for finite volume studies.

Here we concentrate on the scalar (σ) and pseudoscalar (π) channels. These contributions can be written as

$$\Pi_\pi^{ab}(q^2) = \int_\lambda^\Lambda \frac{d^4p}{(2\pi)^4} \, \mathrm{Tr}(i\gamma_5\tau^a S(p+q)i\gamma_5\tau^b S(q))$$

$$\Pi_\sigma(q^2) = \int_\lambda^\Lambda \frac{d^4p}{(2\pi)^4} \, \mathrm{Tr}(S(p+q)S(q)). \tag{15}$$

The pole mass can be obtained by solving

$$1 - 2G_M\Pi^M(\omega = m_M, \vec{q} = 0) = 0, \tag{16}$$

where m_M is the mass of a particular meson. The detailed expression for Π^M and G_M for π and σ mesons may be found in Ref. [43].

In the upper panels of Fig. 9 we have plotted the masses of pion (m_π) and sigma (m_σ) as a function of temperature for different system sizes. In any given volume we see that for low temperatures the masses of pion and sigma are different and they become degenerate above T_c where chiral symmetry is expected to get restored. With decrease in volume we find the pion mass to increase. However above $1.2T_c$ the pion mass for infinite volume suddenly shoots up above those for the finite volumes. This may have important consequences in heavy-ion reactions where system size is small. Whereas for infinite volume the fast
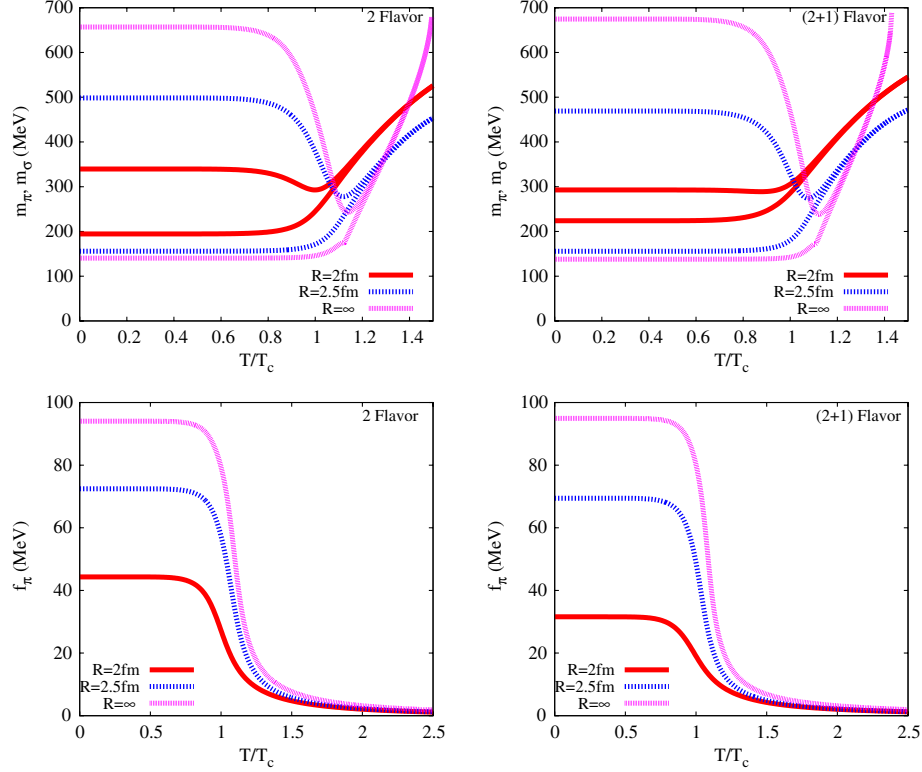
FIG. 9 (color online).   Variation of meson masses (upper panel) and pion decay constant (lower panel) with temperature for different system sizes. In the upper panel the three monotonously rising curves are for m_π and the other three are for m_σ.

increasing mass of pion would drastically reduce the chances of obtaining pion-like bound states, the same may not be true for finite volume. We note here that the increase of pion mass with decreasing volume has also been observed in computations with chiral perturbation theory [57] and renormalization group methods in quark-meson model [58].

While the mass of pion increases with decreasing volume at low temperatures, the mass of sigma is found to decrease quite fast. One can actually see a trend to the masses of the two chiral partners becoming closer to each other with decreasing volume. This, yet again, shows that chiral symmetry breaking effects reduce with decreasing volumes.

The pion decay constant may be obtained from the matrix element $\langle 0|J_{\mu,5}^a|\pi^b(k)\rangle = i\delta_{ab}f_\pi k_\mu$, where $J_{\mu,5}^a = \bar\psi \gamma_\mu \gamma_5 \frac{\tau^a}{2} \psi$ is the chiral current. At finite temperature and for a particular volume it can be written as (see Refs. [32,33] and including the low momentum cut-off λ)

$$f_\pi^2 = \frac{3M_u^2}{2\pi^2}\left[\int_\lambda^\Lambda \frac{p^2 dp}{E_p^3} - 2\int_\lambda^\infty \frac{p^2 dp}{E_p^3} f(E_p)\right], \quad (17)$$

where $E_p = \sqrt{p^2 + M_u^2}$ is the single particle energy of a light quark and $f(E_p)$ is the distribution function properly modified due to Polyakov loop interaction.

As shown in the lower panels of Fig. 9, the pion decay *constant* decreases both with the decrease in temperature and with that of system size. The decrease of f_π with

temperature has also been observed in other effective models [54,59], Dyson-Schwinger approaches [60] as well as in LQCD [61]. This is also an indication of the restoration of chiral symmetry as f_π is directly proportional to the divergence of the chiral current.

The tendency of chiral symmetry getting restored in finite volumes may also be noted by comparing Fig. 9 with Fig. 2. At low temperatures the constituent quark masses decrease with decreasing volume. It so happens that the light constituent quark masses become smaller than the pion mass for the smallest sizes studied here. These quarks should then become thermodynamically more favored than the pions. Though fortunately in the PNJL model, such constituent quarks will be suppressed due to the presence of the Polyakov loop, the pions would still lose their significance as the lightest particles that made them suitable candidates for becoming the Goldstone bosons. Thus what seems to happen is that the decrease of volume restores the spontaneous breaking of chiral symmetry in the same way as increase in temperature. The *critical size* R_c for such symmetry restoration would be somewhere between 2 and 2.5 fm. From Fig. 2 it may be noted that this range of sizes is almost equal to the respective constituent quark masses. This observation is commensurate with the expectation from chiral perturbation theory that chiral symmetry restoration may take place once the quark masses become equal to the inverse of system size [62].
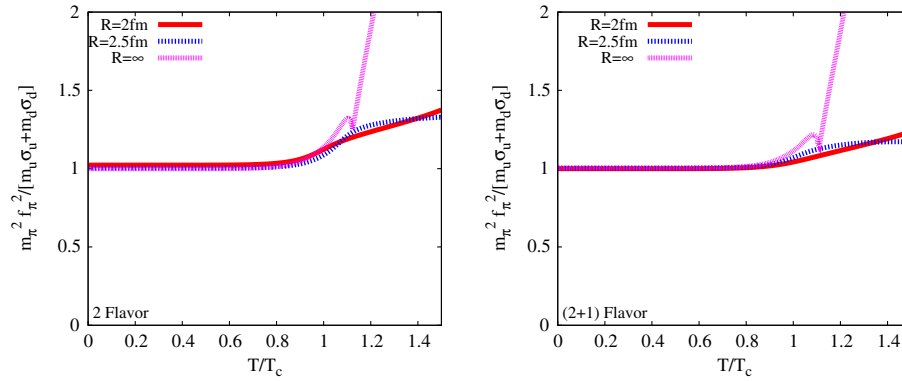
FIG. 10 (color online).   Checking for violation of the GMOR relation as a function of temperature and system size.

With all the strong indication of a possible chiral symmetry restoration with decreasing volume it would be interesting to see what happens to the Gell-Mann Oakes Renner (GMOR) [63] relation, which in the lowest order of chiral expansion is given by $f_\pi^2 m_\pi^2 = m_u \sigma_u + m_d \sigma_d$. Normally with increase in temperature as the spontaneously broken part of the chiral symmetry gets restored the GMOR relation should start to break down. This is exactly what we find in our calculations and shown in Fig. 10. But surprisingly we find that similar effect is not observed for the decrease in volume and the GMOR relation holds good for the all the ranges of volumes we considered almost up to temperatures as high as $0.8 T_c$. In fact even at higher temperatures the GMOR relation is violated the most for infinite volumes. The way one can understand this is that for a physical chiral expansion a quantity $m_\pi / \mathcal{M}$ is required, where $\mathcal{M}$ is some suitable scale. In chiral perturbation theory $\mathcal{M}$ is usually the nucleon mass, in zero temperature NJL or PNJL models it is the high momentum cutoff Λ, etc. For finite temperatures one can then consider T to play the role of $\mathcal{M}$. Thus, given a temperature if the corresponding m_π in a given volume is less than T, chiral identities would work properly (see e.g., Ref. [64]). So here we have a situation where chiral symmetry is getting restored while partial conservation of axial current is still maintained.

VI. CONCLUSION

We have tried to understand the dynamics of strongly interacting matter inside finite volume in the framework of the PNJL model with saddle point approximation. Several interesting results were observed that can have important implications for heavy-ion collision experiments. Our major finding was that the spontaneously broken chiral symmetry may be restored at much lower temperatures in small volume. This was shown through the computation of various thermodynamic observables as well as certain hadron properties.

Changes in the equation of state and speed of sound may have important consequences in the flow properties of the exotic medium created in the experiments. A measure of the specific heat in heavy-ion experiments is the transverse momentum fluctuations. We find the specific heat to decrease with decreasing volume indicating that the momentum fluctuations may not be as large as expected at a given T/T_c.

From the variation of the phase boundary with changing volume we demonstrated a stronger possibility of finding the signatures of a critical endpoint in low energy experiments that intend to create high baryonic densities where the expected temperature is not too high.

Finally from the hadron properties we observed the possibility of obtaining a chiral symmetric but confined phase in small volumes. We hope that a combination of heavy ion collisions and not-so-heavy ion collisions at similar center of mass energies, followed by an appropriate finite size scaling study may give us a better understanding of the QCD phase structure.

As discussed earlier we made a couple of simplified assumptions in this work. The Polyakov loop potential used here does not have an explicit volume dependence. The discrete momentum states in the quark potential was replaced with a continuum, and the only explicit dependence on system size was through the lower momentum cutoff. Though we believe that these assumptions would not affect the gross features observed, we hope to address these issues in future. It would be of highly desirable to have a concurrent study of finite size effects in Polyakov-Quark-Meson models [65] to further understand the systematics of model artifacts.

[1] K. Rajagopal and F. Wilczek, in *At the Frontier of Particle Physics/Handbook of QCD*, edited by M. Shifman (World Scientific, Singapore, 2000), Vol. 3, p. 2061.

[2] E. W. Kolb and M. S. Turner, in *Frontiers in Physics: The Early Universe*, edited by D. Pines (Perseus Books Group, New York, 1994).

[3] A. Bhattacharyya, S. K. Ghosh, S. Majumder, and R. Ray, Phys. Rev. D **86**, 096006 (2012).

[4] D. H. Boal, C.-K. Gelbke, and B. K. Jennings, Rev. Mod. Phys. **62**, 553 (1990).

[5] M. A. Lisa, S. Pratt, R. Soltz, and U. Wiedemann, Annu. Rev. Nucl. Part. Sci. **55**, 357 (2005).

[6] D. Adamova *et al.*, Phys. Rev. Lett. **90**, 022301 (2003).

[7] G. Graef, M. Bleicher, and Q. Li, Phys. Rev. C **85**, 044901 (2012).

[8] S. Bass *et al.*, Prog. Part. Nucl. Phys. **41**, 255 (1998); M. Bleicher *et al.*, J. Phys. G **25**, 1859 (1999); H. Petersen, J. Steinheimer, G. Burau, M. Bleicher, and H. Stöcker, Phys. Rev. C **78**, 044901 (2008).

[9] M. E. Fisher and A. E. Ferdinand, Phys. Rev. Lett. **19**, 169 (1967).

[10] A. E. Ferdinand and M. E. Fisher, Phys. Rev. **185**, 832 (1969); M. E. Fisher and M. N. Barber, Phys. Rev. Lett. **28**, 1516 (1972); M. N. Barber, in *Phase Transitions and Critical Phenomenon*, edited by C. Domb and J. L. Lebowitz (Academic Press, New York, 1987), Vol. 8, p. 146; J. L. Cardy, *Scaling and Renormalization in Statistical Physics* (Cambridge, New York, 1996); D. Amit, *Field Theory; The Renormalization Group and Critical Phenomena* (World Scientific, Singapore, 2005).

[11] L. M. Abreu, M. Gomes, and A. J. da Silva, Phys. Lett. B **642**, 551 (2006).

[12] L. F. Palhares, E. S. Fraga, and T. Kodama, J. Phys. G **38**, 085101 (2011).

[13] E. S. Fraga, L. F. Palhares, and P. Sorensen, Phys. Rev. C **84**, 011903(R) (2011).

[14] H.-T. Elze and W. Greiner, Phys. Lett. B **179**, 385 (1986).

[15] C. Spieles, H. Stoecker, and C. Greiner, Phys. Rev. C **57**, 908 (1998).

[16] A. Gopie and M. C. Ogilvie, Phys. Rev. D **59**, 034009 (1999).

[17] A. Bazavov and B. A. Berg, Phys. Rev. D **76**, 014502 (2007).

[18] C. S. Fischer and M. R. Pennington, Phys. Rev. D **73**, 034029 (2006).

[19] J. Luecker, C. S. Fischer, and R. Williams, Phys. Rev. D **81**, 094005 (2010).

[20] M. Luscher, Commun. Math. Phys. **104**, 177 (1986).

[21] J. Gasser and H. Leutwyler, Phys. Lett. B **188**, 477 (1987).

[22] Y. Nambu and G. Jona-Lasinio, Phys. Rev. **122**, 345 (1961); **124**, 246 (1961).

[23] O. Kiriyama and A. Hosaka, Phys. Rev. D **67**, 085010 (2003).

[24] G. Shao, L. Chang, Y. Liu, and X. Wang, Phys. Rev. D **73**, 076003 (2006).

[25] J. Braun, B. Klein, and P. Piasecki, Eur. Phys. J. C **71**, 1576 (2011).

[26] J. Braun, B. Klein, and B.-J. Schefer, Phys. Lett. B **713**, 216 (2012).

[27] F. C. Khanna, A. P. C. Malbouisson, J. M. C. Malbouisson, and A. E. Santana, Europhys. Lett. **97**, 11002 (2012).

[28] S. Yasui and A. Hosaka, Phys. Rev. D **74**, 054036 (2006).

[29] L. M. Abreu, A. P. C. Malbouisson, and J. M. C. Malbouisson, Phys. Rev. D **83**, 025001 (2011).

[30] L. M. Abreu, A. P. C. Malbouisson, and J. M. C. Malbouisson, Phys. Rev. D **84**, 065036 (2011).

[31] D. Ebert, T. G. Khunjua, K. G. Klimenko, and V. Ch. Zhukovsky, Int. J. Mod. Phys. A **27**, 1250162 (2012).

[32] S. P. Klevansky, Rev. Mod. Phys. **64**, 649 (1992).

[33] T. Hatsuda and T. Kunihiro, Phys. Rep. **247**, 221 (1994).

[34] T. Kunihiro and T. Hatsuda, Phys. Lett. B **206**, 385 (1988).

[35] L. D. McLerran and B. Svetitsky, Phys. Rev. D **24**, 450 (1981); B. Svetitsky and L. G. Yaffe, Nucl. Phys. **B210**, 423 (1982); B. Svetitsky, Phys. Rep. **132**, 1 (1986); R. D. Pisarski, Phys. Rev. D **62**, 111501 (2000); Marseille 2000, Strong and electroweak matter pp. 107–117 (arXiv:hep-ph/0101168); E. Megias, E. Ruiz Arriola, and L. L. Salcedo, Phys. Rev. D **69**, 116003 (2004); D. Diakonov and M. Oswald, Phys. Rev. D **70**, 105016 (2004); A. Dumitru and R. D. Pisarski, Phys. Lett. B **504**, 282 (2001); Phys. Rev. D **66**, 096003 (2002); Nucl. Phys. **A698**, 444 (2002); O. Scavenius, A. Dumitru, and J. T. Lenaghan, Phys. Rev. C **66**, 034903 (2002).

[36] K. Fukushima, Phys. Lett. B **591**, 277 (2004).

[37] C. Ratti, M. A. Thaler, and W. Weise, Phys. Rev. D **73**, 014019 (2006).

[38] E. Megias, E. R. Arriola, and L. L. Salcedo, Phys. Rev. D **74**, 065005 (2006); **74**, 114014 (2006); J. High Energy Phys. 01 (2006) 073.

[39] S. K. Ghosh, T. K. Mukherjee, M. G. Mustafa, and R. Ray, Phys. Rev. D **73**, 114007 (2006); S. Mukherjee, M. G. Mustafa, and R. Ray, Phys. Rev. D **75**, 094015 (2007).

[40] C. Ratti, S. Roessner, and W. Weise, Phys. Lett. B **649**, 57 (2007); C. Roessner, S. Ratti, and W. Weise, Phys. Rev. D **75**, 034007 (2007); S. Roessner, T. Hell, C. Ratti, and W. Weise, Nucl. Phys. **A814**, 118 (2008).

[41] S. K. Ghosh, T. K. Mukherjee, M. G. Mustafa, and R. Ray, Phys. Rev. D **77**, 094024 (2008).

[42] M. Ciminale, R. Gatto, N. D. Ippolito, G. Nardulli, and M. Ruggieri, Phys. Rev. D **77**, 054023 (2008).

[43] P. Deb, A. Bhattacharyya, S. Datta, and S. K. Ghosh, Phys. Rev. C **79**, 055208 (2009).

[44] E. Megias, E. R. Arriola, and L. L. Salcedo, Phys. Rev. Lett. **109**, 151601 (2012).

[45] M. Cristoforetti, T. Hell, B. Klein, and W. Weise, Phys. Rev. D **81**, 114017 (2010).

[46] A. Bhattacharyya, P. Deb, S. K. Ghosh, and R. Ray, Phys. Rev. D **82**, 014021 (2010).

[47] A. Bhattacharyya, P. Deb, A. Lahiri, and R. Ray, Phys. Rev. D **82**, 114028 (2010).

[48] A. Bhattacharyya, P. Deb, A. Lahiri, and R. Ray, Phys. Rev. D **83**, 014001 (2011).

[49] S. Bose, P. Raychaudhuri, R. Banerjee, P. Vasa, and P. Ayyub, Phys. Rev. Lett. **95**, 147003 (2005).

[50] J. C. Collins, A. Duncan, and S. D. Joglekar, Phys. Rev. D **16**, 438 (1977).

[51] N. K. Nielsen, Nucl. Phys. **B120**, 212 (1977).

[52] R. Korus, St. Mrowczynski, M. Rybczynski, and Z. Wlodarczyk, Phys. Rev. C **64**, 054908 (2001).

[53] H. Hansen, W. M. Alberico, A. Beraudo, A. Molinari, M. Nardi, and C. Ratti, Phys. Rev. D **75**, 065004 (2007).

[54] W.-j. Fu and Y.-x. Liu, Phys. Rev. D **79**, 074011 (2009).

[55] P. Costa, M. C. Ruivo, C. A. de Sousa, H. Hansen, and W. M. Alberico, Phys. Rev. D **79**, 116003 (2009).

[56] A. L. Fetter and J. D. Walecka, *Quantum Theory of Many-Particle System* (McGraw-Hill, New York, 1971).

[57] G. Colangelo and S. Durr, Eur. Phys. J. C **33**, 543 (2004); G. Colangelo, S. Durr, and C. Haefeli, Nucl. Phys. **B721**, 136 (2005); G. Colangelo and C. Haefeli, Nucl. Phys. **B744**, 14 (2006).

[58] B. Klein, Few-Body Syst. **53**, 45 (2012).

[59] A. Barducci, R. Casalbuoni, S. De Curtis, R. Gatto, and G. Pettini, Phys. Lett. B **240**, 429 (1990); Phys. Rev. D **42**, 1757 (1990); S. Jeon and J. Kapusta, Phys. Rev. D **54**, 6475 (1996); O. Kiriyama, M. Maruyama, and F. Takagi, Phys. Rev. D **58**, 116001 (1998).

[60] M. Harada and A. Shibata, Phys. Rev. D **59**, 014010 (1998); J. Luecker, C. S. Fischer, and R. Williams, Phys. Rev. D **81**, 094005 (2010).

[61] E. Laermann and F. Pucci, Eur. Phys. J. C **72**, 2200 (2012).

[62] J. Gasser and H. Leutwyler, Nucl. Phys. **B307**, 763 (1988).

[63] M. Gell-Mann, R. J. Oakes, and B. Renner, Phys. Rev. **175**, 2195 (1968).

[64] D. T. Son and M. A. Stephanov, Phys. Rev. D **66**, 076011 (2002).

[65] B.-J. Schaefer, J. M. Pawlowski, and J. Wambach, Phys. Rev. D **76**, 074023 (2007); B.-J. Schaefer, M. Wagner, and J. Wambach, Phys. Rev. D **81**, 074013 (2010).